The Journal of Immunology

TNF Receptor–Associated Factor 5 Limits Function of Plasmacytoid Dendritic Cells by Controlling IFN Regulatory Factor 5 Expression

Shuhei Kobayashi, Tsuyoshi Sakurai, Takanori So, Yuka Shiota, Atsuko Asao, Hai The Phung, Riou Tanaka, Takeshi Kawabe, Takashi Maruyama, Emi Kanno, Kazuyoshi Kawakami, Yuji Owada and Naoto Ishii

J Immunol 2019; 203:1447-1456; Prepublished online 16 August 2019;
doi: 10.4049/jimmunol.1900188
http://www.jimmunol.org/content/203/6/1447

The Journal of Immunology is published twice each month by
The American Association of Immunologists, Inc.,
1451 Rockville Pike, Suite 650, Rockville, MD 20852

Print ISSN: 0022-1767 Online ISSN: 1550-6606.

TNF Receptor–Associated Factor 5 Limits Function of Plasmacytoid Dendritic Cells by Controlling IFN Regulatory Factor 5 Expression

Shuhei Kobayashi,* Tsuyoshi Sakurai,* Takanori So,*,† Yuka Shiota,* Atsuko Asao,* Hai The Phung,* Riou Tanaka,* Takeshi Kawabe,* Takashi Maruyama,‡ Emi Kanno,§ Kazuyoshi Kawakami,¶ Yuji Owada,‖ and Naoto Ishii*

The physiological functions of TNF receptor–associated factor 5 (TRAF5) in the skin inflammation and wound healing process are not well characterized. We found that *Traf5*$^{-/-}$ mice exhibited an accelerated skin wound healing as compared with wild-type counterparts. The augmented wound closure in *Traf5*$^{-/-}$ mice was associated with a massive accumulation of plasmacytoid dendritic cells (pDCs) into skin wounds and an enhanced expression of genes related to wound repair at skin sites. In accordance with this result, adoptive transfer of *Traf5*$^{-/-}$ pDCs, but not wild-type pDCs, into the injured skin area in wild-type recipient mice significantly promoted skin wound healing. The expression of skin-tropic chemokine receptor CXCR3 was significantly upregulated in *Traf5*$^{-/-}$ pDCs, and treatment with a CXCR3 inhibitor cancelled the promoted wound healing in *Traf5*$^{-/-}$ mice, suggesting a pivotal role of CXCR3 in pDC-dependent wound healing. *Traf5*$^{-/-}$ pDCs displayed significantly higher expression of IFN regulatory factor 5 (IRF5), which correlated with greater induction of proinflammatory cytokine genes and CXCR3 protein after stimulation with TLR ligands. Consistently, transduction of exogeneous TRAF5 in *Traf5*$^{-/-}$ pDCs normalized the levels of abnormally elevated proinflammatory molecules, including IRF5 and CXCR3. Furthermore, knockdown of IRF5 also rescued the abnormal phenotypes of *Traf5*$^{-/-}$ pDCs. Therefore, the higher expression and induction of IRF5 in *Traf5*$^{-/-}$ pDCs causes proinflammatory and skin-tropic characteristics of the pDCs, which may accelerate skin wound healing responses. Collectively, our results uncover a novel role of TRAF5 in skin wound healing that is mediated by IRF5-dependent function of pDCs. *The Journal of Immunology*, 2019, 203: 1447–1456.

The skin is a barrier that protects the host from external threats, including microbial infections and trauma. Upon acute skin injury, the cellular components of the immune system, the blood coagulation and inflammatory pathways are activated and coordinated to restore the tissue integrity and homeostasis (1). Skin resident and infiltrating cells, including neutrophils, monocytes, lymphocytes, dendritic cells, endothelial cells, keratinocytes, and fibroblasts, work together and react rapidly to the stimulus, and this event immediately initiates wound repair and regeneration responses (1–3). In particular, inflammatory responses mediated by immune cells play important roles in wound healing (4, 5). However, because skin wound healing processes involve too many cell/cell networks spatiotemporally, the precise molecular mechanisms remain unclear.

Plasmacytoid dendritic cells (pDCs) are a small cell population in the periphery and are identified as cells producing large amounts of type I IFNs in response to viral infections (6–9). These cells specially equip endosomal TLR7 and TLR9 that recognize virus- and host-derived nucleic acids (9–11). TLR-mediated activation of pDCs plays a pivotal role for protective immunity, whereas excessive activation of pDCs gives rise to autoimmune diseases, such as systemic lupus erythematosus and psoriasis (9–15). Additionally, self-nucleic acids released from the damaged tissues in the presence of an antimicrobial peptide activate pDCs to induce type I IFN responses that drive autoimmunity in psoriasis (10, 15). Thus, it is considered that pDCs may play important roles in the regulation of tissue homeostasis in the skin. Although a previous study reported that pDCs sensed tissue damage and promoted skin wound healing through the secretion of type I IFNs (16), it is still unknown how pDCs are regulated during skin wound healing.

In this study, we found that *Traf5*$^{-/-}$ mice showed a massive infiltration of pDCs into injured skin tissues. Adoptive transfer of *Traf5*$^{-/-}$ pDCs into the skin of wild-type mice led to acceleration of skin wound healing. In addition, *Traf5*$^{-/-}$ pDCs showed a significant increase in proinflammatory cytokines and skin-tropic chemokine receptor CXCR3 in comparison with wild-type pDCs. Inhibition of CXCR3 function restored the accelerated skin wound healing in *Traf5*$^{-/-}$ mice, suggesting a critical role of CXCR3. Upon

*Department of Microbiology and Immunology, Graduate School of Medicine, Tohoku University, Sendai 980-8575, Japan; †Laboratory of Molecular Cell Biology, Graduate School of Medicine and Pharmaceutical Sciences, University of Toyama, Toyama 930-0194, Japan; ‡Department of Immunology, Graduate School of Medicine and Faculty of Medicine, Akita University, Akita 010-8543, Japan; §Department of Science of Nursing Practice, Graduate School of Medicine, Tohoku University, Sendai 980-8575, Japan; ¶Department of Medical Microbiology, Mycology and Immunology, Graduate School of Medicine, Tohoku University, Sendai 980-8575, Japan; and ‖Department of Organ Anatomy, Graduate School of Medicine, Tohoku University, Sendai 980-8575, Japan

ORCIDs: 0000-0002-0439-2588 (H.T.P.); 0000-0003-0820-3219 (T.M.); 0000-0003-2339-122X (E.K.).

Received for publication February 14, 2019. Accepted for publication July 19, 2019.

This work was supported by Japan Society for the Promotion of Science KAKENHI Grants 16K15508 (to N.I.), JP15H04640 (to T. So), and JP18H02572 (to T. So).

Address correspondence and reprint requests to Prof. Naoto Ishii, Department of Microbiology and Immunology, Graduate School of Medicine, Tohoku University, 2-1 Seiryo-machi, Aoba-ku, Sendai 980-8575, Japan. E-mail address: ishiin@med.tohoku.ac.jp

The online version of this article contains supplemental material.

Abbreviations used in this article: Col1α1, collagen type I, α 1; IRF5, IFN regulatory transcription factor 5; KRT5, keratin 5; pDC, plasmacytoid dendritic cell; α-SMA, α–smooth muscle actin.

stimulation with TLR agonists in vitro, *Traf5*$^{-/-}$ pDCs produced higher levels of inflammatory cytokines and CXCR3 accompanied by enhanced nuclear accumulation of IFN regulatory transcription factor 5 (IRF5). The transduction of TRAF5 restored the expression of CXCR3 in *Traf5*$^{-/-}$ pDCs, and short hairpin RNA–mediated knockdown of IRF5 significantly corrected the enhanced expression of CXCR3, implying that TRAF5 may limit CXCR3 expression via IRF5. To our knowledge, our study first reveals a critical function of TRAF5 for the regulation of pDCs in the process of skin wound healing.

Materials and Methods

Mice

Traf5$^{-/-}$ mice on a C57BL/6 background have been described (17). All mice were bred and maintained under specific pathogen-free conditions, and experiments were in compliance with protocols approved by the Institute for Animal Experimentation, Tohoku University Graduate School of Medicine (2018MdA-190).

Bone marrow transplantation

Irradiated wild-type and *Traf5*$^{-/-}$ mice (9.5 Gy) at age of 6 wk were used as recipients for transplantation. To obtain donor cells, the femurs and tibias were collected aseptically from euthanized mice, and the bone marrow was washed out with sterile RPMI 1640. Recipient mice were given i.v. injection of 5×10^6 donor bone marrow cells via tail vein and were checked the proportion of donor cells in later time points. Eight weeks after transplantation, mice were used for experiments.

Wound creation and tissue collection

The dorsal hair of anesthetized mice was shaved to fully expose the skin, and then the skin was rinsed with 70% ethanol. Six full-thickness wounds extending to the panniculus carnosus (depth of ~1 mm from the dorsal surface of the skin), at least 5 mm apart, were created on each mouse using a 3-mm-diameter biopsy punch under sterile conditions. The injured areas were covered with a polyurethane film (3M Health Care, St. Paul, MN) and an elastic adhesive bandage (Hilate, Iwatsuki, Tokyo, Japan) as an occlusive dressing. The day when the wounds were made was designated as day 0. At various time points, mice were sacrificed, and the wound tissue was collected by excising the tissue using an 8-mm-diameter biopsy punch. The tissue was used for histological, gene expression, and flow-cytometric analyses. For histological analysis, the skins were fixed with 10% formalin and embedded in paraffin. Sections, 5 μm in thickness, were stained with H&E.

Measurement of the wound area

At various time points, the wounds were photographed. The wound area was quantified by calculating the pixel area using ImageJ software. Percentage of wound closure was calculated using the following formula: % closure of wound area = (1.0 − wound area at the indicated time point/wound area on day 0) × 100. For histological analysis, the area of granulation tissues was measured on these H&E-stained sections and was evaluated by calculating the pixel area. Granulation region was determined by thin collagen and narrow vessels, because thick collagen bundle is usually observed in the dermis of normal unwounded skin.

Isolation of immune cells in the wound tissue

For isolation of cells in the wound tissue, mice were sacrificed before or 3, 6, 24, 48, and 72 h after wounding. The wound tissue was excised using an 8-mm-diameter biopsy punch and teased apart using stainless steel mesh. Minced wound tissues were digested with 1 mg/ml collagenase (Sigma-Aldrich, St. Louis, MO), 500 μg/ml DNase (Sigma-Aldrich), 1 mg/ml hyaluronidase (Sigma-Aldrich), and 1 mg/ml dispase (Roche Diagnostics, Tokyo, Japan) in RPMI 1640 medium at 37°C for 90 min. The tissue homogenate was disaggregated by vigorous pipetting, and single-cell suspension was prepared by filtrating through a 40-μm cell strainer. The isolated cells were evaluated by flow cytometry.

Trans-*well migration assay*

Polycarbonate membrane inserts with 5-μm pore size (Corning-Costar, Lowell, MA) were used. For pDC migration, wild-type mouse embryonic fibroblast cells were initially cultured in the lower well, then stimulated with IFN-γ to induce CXCL chemokines. Splenic pDCs (PDCA-1$^+$B220$^+$CD11c^{int}Ly-6C$^+$) (2×10^4 cells per well) isolated from wild-type or *Traf5*$^{-/-}$ mice were suspended in RPMI 1640 medium containing 1% FBS and incubated at 37°C for 2 h in the presence or absence of AMG487, and then pDCs were placed and cultured for 3 h in the upper chambers. The number of migrated pDCs in the lower chambers were evaluated by flow cytometry.

Lentiviral transduction into bone marrow cells

The lentiviral vector for exogenous TRAF5 expression was constructed by inserting mouse *Traf5* cDNA into the CS2 vector (Riken). For IRF5 gene knockdown, the lentiviral vector construct was previously described (18). The lentiviral vectors were transiently transfected into HEK293T cells along with packaging plasmids (pCAG-HIVgp), virus-containing media were harvested at 48 h after transfection. Virus-containing supernatants were concentrated by centrifugation at 6000 × *g* at 4°C for 16 h, and then the concentrated virus particles was added into bone marrow cells from *Traf5*$^{-/-}$ mice in the presence of 8 μg/ml polybrene.

Culture of bone marrow–derived pDCs

One day after lentiviral infection, virus-containing media were removed from the bone marrow cell culture and replaced with a pDC differentiation medium supplemented with Flt3 ligand (50 ng/ml). On day 3, GFP$^+$ cells were sorted by FACS and further cultured for 5 d to differentiate into PDCA-1$^+$B220$^+$CD11c^{int}Ly-6C$^+$ cells as pDCs.

s.c. Adoptive transfer

Peritoneal macrophages (CD11b$^+$F4/80$^+$) and splenic pDCs (PDCA-1$^+$B220$^+$CD11c^{int}Ly-6C$^+$) were isolated from wild-type and *Traf5*$^{-/-}$ mice and then were independently s.c. transferred (2.0×10^6 cells) into the wound area on wild-type mice.

Peptide, chemicals, Abs, and cytokines

APC-conjugated anti-mouse CD3 (17A2), APC-conjugated anti-mouse CD8α (53-6.7), APC-conjugated anti-mouse/human CD45R/B220 (RA3-6B2), APC-conjugated anti-mouse CD45.2 (104), PE-conjugated anti-mouse CD8α (53-6.7), PE-conjugated anti-mouse CD11b (M1/70), PE-conjugated anti-mouse CD45 (30-F11), PE-conjugated anti-mouse CD45.1 (A20), PE-conjugated anti-mouse CD183 (CXCR3-173), PE-conjugated anti-mouse CD317 (BST2, PDCA-1) (927), FITC-conjugated anti-mouse CD11c (N418), FITC-conjugated anti-mouse Ly-6G/Ly-6C (Gr.1) (RB6-8C5), FITC-conjugated anti-mouse TCR-γ/δ (GL3), FITC-conjugated anti-mouse CD45 (30-F11), Pacific Blue–conjugated anti-mouse CD4 (GK1.5), Pacific Blue–conjugated anti-mouse CD317 (BST2, PDCA-1) (927), and Brilliant Violet 421 anti-mouse F4/80 (BM8) Abs were purchased from BioLegend (San Diego, CA). APC Annexin V was purchased from BioLegend. PE-conjugated anti-mouse IL-6 (MP5-20F3) and PE Ki67 (SolA15) Abs were obtained from eBioscience (San Diego, CA). PE rat anti-mouse TNF (MP6-XT22) Ab was obtained from BD Biosciences (San Jose, CA). Biotinylated anti-mouse Siglec-H (440c) was obtained from Hycult Biotech (Canton, MA). Mouse rIFN-γ was obtained from PeproTech (Rocky Hill, NJ). AMG487 was obtained from Tocris Bioscience (Bristol, U.K.). CpG oligodeoxynucleotide was purchased from InvivoGen (San Diego, CA), and R848 peptide was purchased from Enzo Life Sciences (New York, NY). Anti–IκB-α (C-21), anti-ERK1/2 (C-14), anti-p38 (C-20), and anti-JNK (C-17) were purchased from Santa Cruz Biotechnology (Dallas, TX). Anti–phospho-ERK1/2 (E10), anti–phospho-p38 MAPK (D3F9), and anti–phospho-JNK (81E11) were purchased from Cell Signaling Technology (Danvers, MA). Anti–β-actin (C4; MAB1501) was from MilliporeSigma.

RNA extraction and real-time RT-PCR

SYBR Premix Ex Tag (Takara Bio) and a 7500 real-time PCR system (Life Technologies) were used for quantitative RT-PCR. Total RNA was extracted with RNAiso Plus (Life Technologies), and cDNA was then synthesized with SuperScript III Reverse Transcriptase and oligo(dT)20 (Life Technologies). Each transcript was analyzed concurrently on the same plate with the gene encoding GAPDH, and results are presented relative to the abundance of transcripts encoding GAPDH. The primer sequences used were commonly described elsewhere.

Flow cytometry

Cells were incubated with anti-CD16/CD32 (2.4G2; produced in-house) before being stained with the appropriate Abs to cell-surface and intracellular Ags. For intracellular staining, after cell activation with TLR agonists and staining of surface markers, cells were fixed and permeabilized with Cytofix/Cytoperm and Perm/Wash buffer (BD Biosciences) or Foxp3 staining buffer (Affymetrix) according to the manufacturer's instructions.

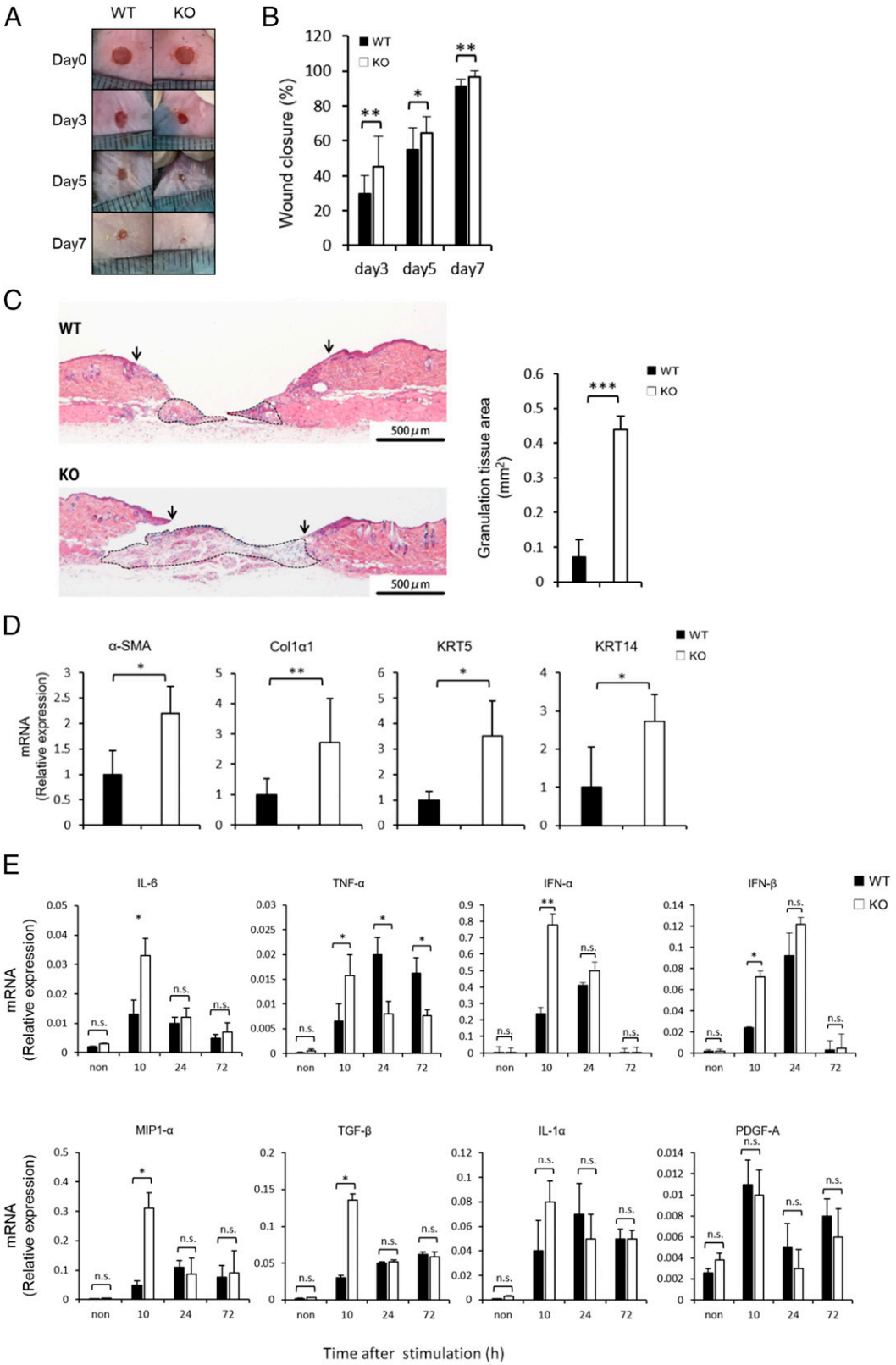

FIGURE 1. TRAF5 limits wound healing responses. (**A**) Wound photographs of wild-type (WT) and *Traf5*$^{-/-}$ knockout (KO) mice. Representative results from three independent experiments with at least three animals in each group are shown. (**B**) Percentages of the wound closure in WT and KO mice after wounding on days 3, 5, and 7. (**C**) Representative histological views (H&E) of skin wounds on day 3 (left panel). Arrows and the dotted line indicate the re-epithelialized leading edges and granulation area, respectively. The area of granulation tissue on H&E-stained sections was measured by calculating the pixel area, as described in the *Materials and Methods* section. (**D**) Expression of α-SMA, Col1α1, KRT5, and KRT14 mRNAs in wound tissues at 72 h after wound injury. (**E**) Expression of IL-6, TNF-α, IFN-α, IFN-β, MIP-1α, TGF-β, IL-1α, and PDGF-A mRNAs in wound tissues at the indicated time points. Data are from three (B) or two (C) pooled experiments or are from one experiment representative of at least three independent experiments with similar results (D and E) [mean ± SEM of nine mice per genotype (total 54 wounds) (B); mean ± SD of seven mice per genotype (C); mean ± SEM of three replicates (D and E)]. *$p < 0.05$, **$p < 0.01$, ***$p < 0.001$ by Student t test.

Data were acquired on a SPECTRAL CELL ANALYZER SP6800 (Sony) or a FACSCanto II (BD Biosciences) and were analyzed with FlowJo software (Tree Star).

Statistical analysis

Statistics were analyzed using Student *t* test (two-tailed), and one-way ANOVA was used to test differences between groups for continuous variables. A p value < 0.05 (indicated as $*p < 0.05$, $**p < 0.01$, and $***p < 0.001$ in the figure legends) was considered statistically significant.

Results

TRAF5 deficiency promotes wound healing in the skin

To understand how TRAF5 controls the wound healing process in the skin, we first examined the rate of wound closure in back skin after full-thickness injury (19, 20). Wound closure was significantly accelerated in *Traf5*$^{-/-}$ mice compared with wild-type mice on days 3, 5, and 7 (Fig. 1A, 1B). Next, to determine the effects on granulation tissue formation, which is mainly comprised of new vessels and novel collagen deposition, and those on the wound depth, we conducted a histological analysis of the wound tissues. In *Traf5*$^{-/-}$ mice, the granulation tissues were markedly well developed compared with those in wild-type mice on day 3 (Fig. 1C). In accordance with enhanced wound closure in *Traf5*$^{-/-}$ mice, keratin 5 (KRT5) and KRT14, which are associated with physiological keratinocyte cell proliferation, were significantly increased on day 3 in *Traf5*$^{-/-}$ mice (Fig. 1D). Collagen type I, α 1 (Col1α1) and α–smooth muscle actin (α-SMA), which are related to granulation tissue formation and myofibroblast differentiation, were also significantly elevated on day 3 in *Traf5*$^{-/-}$ mice (Fig. 1D). The expression of proinflammatory cytokines and chemokines, including IL-6, TNF-α, IFN-α, IFN-β, and MIP-1α (CCL3), was significantly higher at early time points in *Traf5*$^{-/-}$ mice than in wild-type mice (Fig. 1E). Additionally, TGF-β, which is an important factor involved in tissue regeneration by promoting the construction of granulation tissue (3, 21, 22), was also increased in *Traf5*$^{-/-}$ mice (Fig. 1E). However, there was no significant difference in the expression of IL-1α, platelet-derived growth factor–A, keratinocyte chemoattractant, and vascular endothelial growth factor between these two groups (Fig. 1E; data not shown). These results demonstrate that TRAF5 negatively controls skin wound closure probably by suppressing inflammatory responses.

TRAF5 deficiency in hematopoietic cells is important for early wound healing

To evaluate which type of cells are responsible for the accelerated wound healing, we measured *Traf5* mRNA expression in various tissues. We found that the level of *Traf5* mRNA in the skin was relatively lower than that in some other tissues (Supplemental Fig. 1A). Thus, we decided to do a bone marrow transplantation experiment. Bone marrow donor cells from wild-type or *Traf5*$^{-/-}$ mice were transplanted into lethally irradiated wild-type or *Traf5*$^{-/-}$ recipient mice (Fig. 2A), and a full-thickness injury in the back skin was produced in recipient mice to measure the ratio of wound closure. The wound closure was significantly promoted by the transplantation of *Traf5*$^{-/-}$ bone marrow cells, regardless of genotypes of recipient mice (Fig. 2B). In addition, the expression of genes involved in wound healing process, including α-SMA, Col1α1, KRT5, and KRT14, was increased by the transplantation of *Traf5*$^{-/-}$ donor cells (Fig. 2C). α-SMA, Col1α1, and KRT5 are biological markers for angiogenesis, fibroblast activation, and keratinocyte proliferation, respectively. Thus, TRAF5 deficiency in hematopoietic cells plays a dominant role for the accelerated wound healing in recipient mice.

Elevated infiltration of pDC into injured skin of TRAF5-deficient mice

Next, to identify which hematopoietic cells are responsible for the enhanced wound closure in *Traf5*$^{-/-}$ mice, we analyzed cell populations accumulated in wound tissues. At early time points after wounding, significantly higher numbers of hematopoietic cells were accumulated in the skin of *Traf5*$^{-/-}$ mice (Fig. 3A). We found that the accumulation of pDCs, macrophages, CD3^{+} cells,

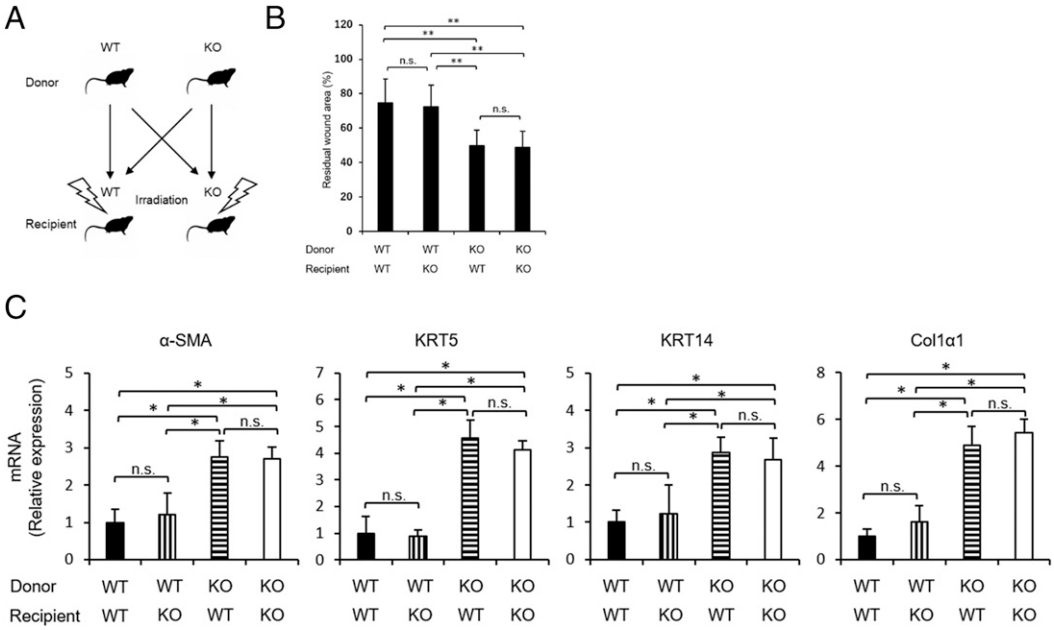

FIGURE 2. TRAF5 in hematopoietic cells is important for wound healing. (**A**) Schematic diagram of a bone marrow transplantation model. (**B**) Percentages of the residual wound area in bone marrow-transplanted recipient mice on day 3 after wounding. (**C**) Expression of α-SMA, Col1α1, KRT5, and KRT14 mRNAs in wound tissues at 72 h after wound injury. Data are from two pooled experiments (B) or are from one experiment representative of at least three independent experiments with similar results (C) [mean ± SEM of eight mice per genotype (total 48 wounds) (B); mean ± SEM of three replicates (C)]. $*p < 0.05$, $**p < 0.01$ by Student *t* test.

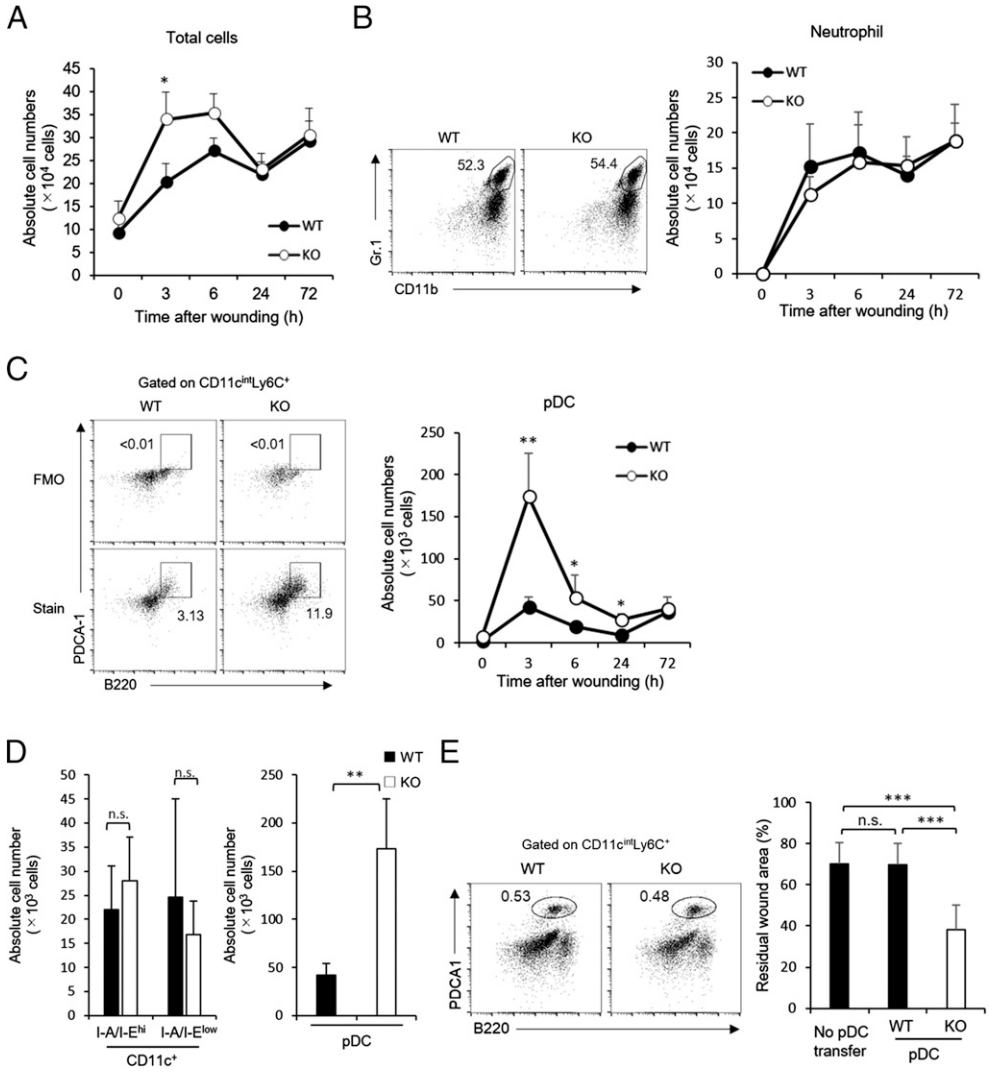

FIGURE 3. Increased infiltration of pDCs into injured skin of TRAF5-deficient mice. (**A–C**) Cell counts of total CD45$^+$ hematopoietic cells (A), neutrophils (B), and pDCs (C) in wound tissues from wild-type (WT) and knockout (KO) mice at the indicated time points after wounding. Numbers adjacent to the outline areas indicate percentage of neutrophils (CD11b$^+$Gr.1$^+$) and pDCs (PDCA-1$^+$B220$^+$CD11c^{int}Ly-6C$^+$). Staining with B220, CD11c, and Ly-6C Abs was used as fluorescence minus one control (FMO), and full staining was made by adding PDCA1 Ab staining. (**D**) Cell count of CD11c$^+$I-A/I-E^{hi} cells, CD11c$^+$I-A/I-E^{low} cells, and pDCs in the wound area of WT and KO mice at 3 h after wounding. (**E**) Gating strategy of splenic pDC (PDCA-1$^+$B220$^+$CD11c^{int}Ly-6C$^+$) isolation (left) and percentages of residual wound area in WT and KO mice on day 3 after wounding under the condition of s.c. WT or KO pDC transfer (right). Data are from three (A and B) or two (C) pooled experiments [mean ± SEM of nine mice per genotype (A and B); mean ± SEM of eight mice per genotype (total 48 wounds) (C)]. $*p < 0.05$, $**p < 0.01$, $***p < 0.001$ by Student t test.

γ/δ T cells, but not neutrophils and conventional dendritic cells, were significantly higher in *Traf5*$^{-/-}$ mice as compared with wild-type mice (Fig. 3B–D, Supplemental Figs. 1B, 3A, 3B). To examine the role of CD3$^+$ cells, we injected anti-CD3 mAb into *Traf5*$^{-/-}$ and wild-type mice to deplete CD3$^+$ cells and confirmed effective depletion of CD3$^+$ cells in the spleen and skin tissues from wild-type and *Traf5*$^{-/-}$ mice (Supplemental Fig. 2A, 2B). In the absence of CD3$^+$ cells, we observed no significant reduction in wound closure (Supplemental Fig. 2C), indicating that infiltrating CD3$^+$ cells in the skin have no major role in healing processes at the early phase of wounding. Similarly, to evaluate the role of macrophages in wound healing responses, we transferred wild-type or *Traf5*$^{-/-}$ peritoneal macrophages into the wounded skin of wild-type recipient mice. Although transfer of *Traf5*$^{-/-}$ macrophages appeared to promote the wound closure compared with wild-type macrophages, transferred *Traf5*$^{-/-}$ macrophages could not promote the wound healing in wild-type mice (Supplemental Fig. 2D), suggesting that accumulated macrophages do not have a critical effect in healing processes at the early phase.

Finally, to examine the role of pDCs in wound healing responses, we adoptively transferred wild-type or *Traf5*$^{-/-}$ pDCs into the skin of wild-type recipient mice. Recipient mice with *Traf5*$^{-/-}$ pDCs led to acceleration of skin wound closure as compared with recipient mice with wild-type pDCs and without pDC transfer (Fig. 3E). These results suggest that rapid and enhanced accumulating pDCs are responsible for the accelerated wound healing observed in *Traf5*$^{-/-}$ mice.

The increased expression of CXCR3 on pDCs in TRAF5-deficient mice

It is known that the expression of skin-tropic chemokine receptors plays an important role in cell infiltration to inflamed skin (23–25). In the steady-state of nonwounded skin tissues, we observed comparable small numbers of pDCs from wild-type and *Traf5*$^{-/-}$ mice (day 0 in Fig. 3C). We thus hypothesized that the capacity of

chemotaxis in *Traf5*$^{-/-}$ pDCs might be enhanced after wounding. We therefore measured the mRNA expression of chemokine receptors in pDCs from wild-type and *Traf5*$^{-/-}$ mice and found that the skin-tropic chemokine receptor CXCR3, which is important for migratory function of pDCs (26–28), was more highly expressed in *Traf5*$^{-/-}$ pDCs than in wild-type pDCs (Fig. 4A). In contrast, CCR2, CCR5, and CCR10, which are also important chemokine receptors for cell migration into inflamed skin tissues, were comparably expressed in wild-type and *Traf5*$^{-/-}$ pDCs (Fig. 4A). Indeed, the expression level of CXCR3 on *Traf5*$^{-/-}$ pDCs and CXCR3^{+} cell ratio in the pDCs were significantly higher than those in wild-type pDCs (Fig. 4B, 4C), suggesting that the expression of CXCR3 on pDCs is functionally relevant for wound healing. To address it, we performed a *trans*-well migration assay that is dependent on CXCL chemokines induced by IFN-γ. The migration capacity of *Traf5*$^{-/-}$ pDCs was significantly higher than that of wild-type pDCs, and the addition of CXCR3 inhibitor AMG487 strongly blocked the cell migration in both wild-type and *Traf5*$^{-/-}$ pDCs (Fig. 4D). Importantly, wild-type and *Traf5*$^{-/-}$ mice treated with AMG487 displayed impaired wound closure (Fig. 4E), showing that CXCR3-driven recruitment of pDCs into wound skin plays a critical role for wound healing responses and that the higher expression of CXCR3 on *Traf5*$^{-/-}$ pDCs may facilitate the accelerated wound closure in *Traf5*$^{-/-}$ mice.

TRAF5 deficiency in pDC promotes TLR-mediated inflammatory responses

pDCs recognize not only viral nucleotides but also self-nucleotides from injured tissues through the TLR7 and TLR9 (7–9). Thus, it might be possible that *Traf5*$^{-/-}$ pDCs in injured skin produce greater amounts of cytokines that promote wound healing and accelerate wound repair at skin. We first measured the gene expression levels of TLR7 and TLR9 in pDCs from wild-type and *Traf5*$^{-/-}$ mice but found no difference (Fig. 5A). Second, to examine whether TRAF5 limits signaling activity of TLR7 and TLR9 in pDCs, pDCs were purified from spleen of naive wild-type and *Traf5*$^{-/-}$ mice and were stimulated with R848 (TLR7 ligand) or CpG DNA (TLR9 ligand). Although TRAF5 deficiency did not affect the proliferation and survival of pDCs (Supplemental Fig. 4A), *Traf5*$^{-/-}$ pDCs markedly upregulated the expression of proinflammatory genes including IL-6, TNF-α, IFN-α, and IFN-β in response to R848 or CpG (Fig. 5B, 5C). These results suggest that TRAF5 may inhibit the signaling activity of TLR7 and TLR9 in pDCs that plays a critical role for producing elevated amounts of inflammatory cytokines required for the skin repair. In addition,

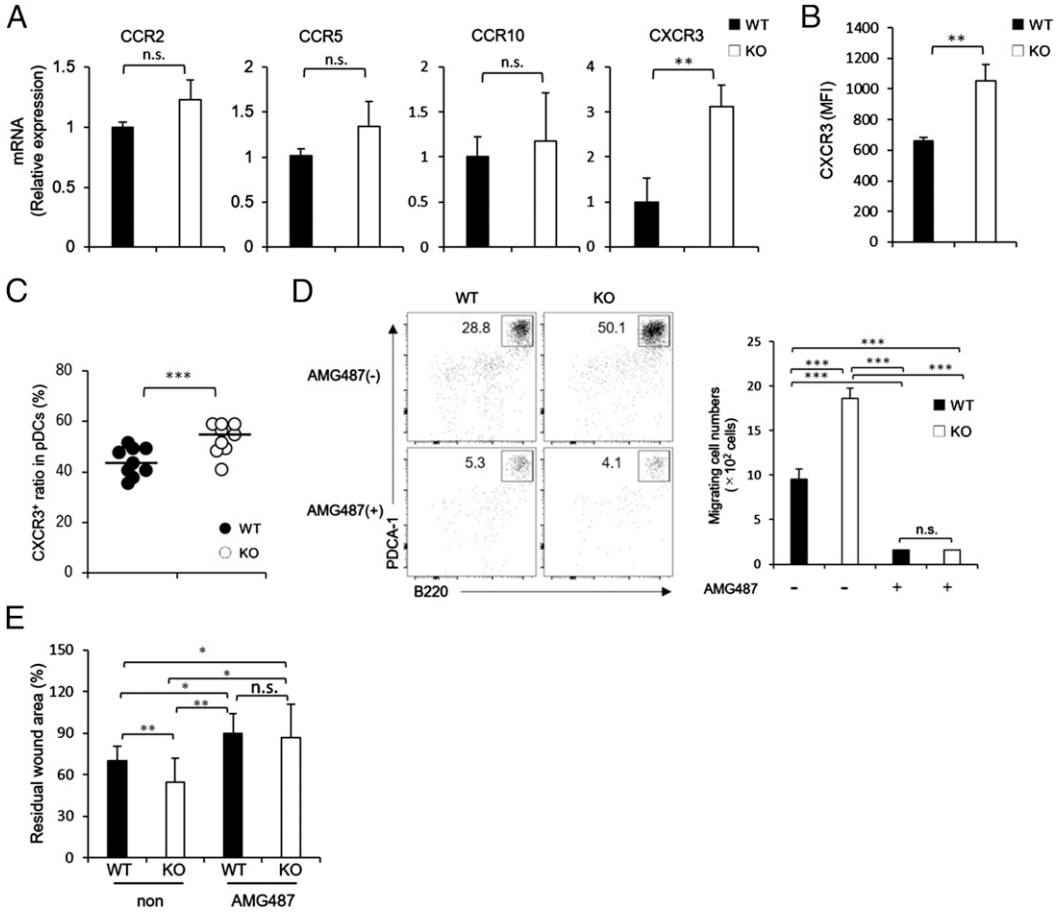

FIGURE 4. TRAF5-deficient pDCs express higher levels of CXCR3. (**A**) Expression of CCR2, CCR5, CCR10, and CXCR3 mRNAs in splenic pDCs from steady-state wild-type (WT) and knockout (KO) mice. (**B** and **C**) Mean fluorescence intensity of CXCR3 on WT and KO splenic pDCs (B) and proportion of CXCR3^{+} pDCs (C). (**D**) Flow cytometric analysis of the extent of postmigrating WT and KO pDCs (PDCA-1^{+}B220^{+}CD11c^{int}Ly-6C^{+}) in *trans*-well assay in the presence or absence of AMG487 (specific inhibitor of CXCR3). Numbers adjacent to the outline areas indicate percentage of pDCs. (**E**) Percentages of residual wound area in WT and KO mice on day 3 after wounding in the presence or absence of AMG487. Data are from one experiment representative of at least three independent experiments with similar results (A, B, and D) or from three pooled experiments (C and E) [mean ± SEM of three replicates (A, B, and D); mean ± SEM of nine mice per genotype (C); mean ± SEM of nine mice per genotype (total 54 wounds) (E)]. *$p < 0.05$, **$p < 0.01$, ***$p < 0.001$ by Student *t* test.

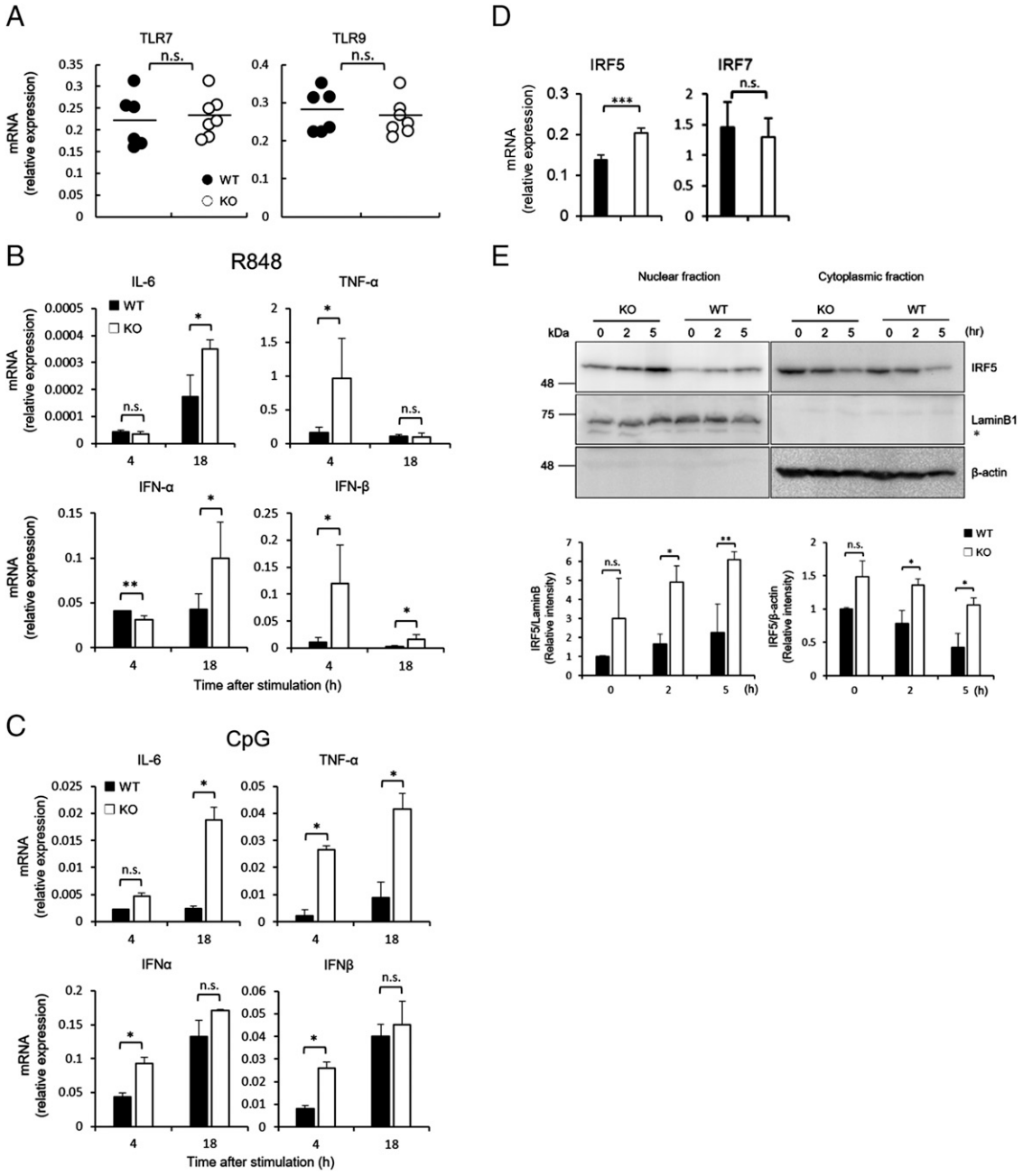

FIGURE 5. Enhanced TLR responses in TRAF5-deficient pDCs. (**A**) Expression of TLR7 and TLR9 mRNAs in splenic pDCs (PDCA-1$^+$B220$^+$CD11c^{int}Ly-6C$^+$) from wild-type (WT) and knockout (KO) mice. (**B** and **C**) Expression of IL-6, TNF-α, IFN-α, and IFN-β mRNAs in WT and KO pDCs after stimulation with 1 μg/ml of R848 (B) or 5 μg/ml of CpG (C). (**D**) Expression of IRF5 and IRF7 mRNAs in splenic pDCs from WT and KO mice. (**E**) Immunoblot analysis of IRF5, LaminB1, and β-actin in WT and KO splenic pDCs stimulated with 5 μg/ml of CpG for the indicated times. Data are from two pooled experiments (A) or one experiment representative of at least three independent experiments with similar results (B–D) [mean ± SEM of seven mice per genotype (A); mean ± SEM of three replicates (B–D)]. $*p < 0.05$, $**p < 0.01$, $***p < 0.001$ by Student t test.

TRAF5 deficiency did not affect the canonical NF-κB pathway induced by CpG as measured by the degradation of IκBα (Supplemental Fig. 4B). Therefore, TRAF5 may negatively control a specific signaling pathway downstream of TLRs in pDCs that is critical for inflammatory cytokine induction and is different from the canonical NF-κB pathway.

IRFs play a pivotal role for induction of proinflammatory cytokines in innate immune responses (29). In particular, IRF5 and IRF7 are important factors to induce inflammatory responses downstream of TLR7 and TLR9 (30–35). Previous studies showed that *Irf5*$^{-/-}$ bone marrow–derived dendritic cells produced lesser amount of proinflammatory cytokines, including IL-6, TNF-α, and type I IFN after ligation of TLRs (31, 33). We thus examined the expression of IRF5 and IRF7 in pDCs. Importantly, quantitative RT-PCR analysis demonstrated that *Traf5*$^{-/-}$ pDCs displayed significantly larger amounts of IRF5 mRNA than did wild-type pDCs (Fig. 5D). However, no significant change in IRF7 was observed between wild-type and *Traf5*$^{-/-}$ groups (Fig. 5D).

IRF5 is predominantly located in the cytoplasm in resting cells and translocates into the nucleus to activate gene transcription upon certain stimulations (29). Indeed, IRF5 protein significantly accumulated in the nucleus of *Traf5*$^{-/-}$ pDCs after stimulation with CpG (Fig. 5E). Therefore, the total and nuclear expression levels of IRF5 are negatively controlled by TRAF5 in pDCs.

Upregulated proinflammatory and skin-tropic characteristics of Traf5$^{-/-}$ pDCs are dependent on IRF5

The in vitro results showed that TRAF5 deficiency caused TLR-driven hyperactivation accompanied by higher expression and activation of IRF5. To examine the mechanism, we prepared TRAF5-expressing *Traf5*$^{-/-}$ pDC from *Traf5*$^{-/-}$ bone marrow cells that were exogenously transduced with *Traf5* cDNA by using a lentiviral vector and then examined the expression levels of proinflammatory cytokines and CXCR3 after stimulation with CpG. The expression of TRAF5 in *Traf5*$^{-/-}$ pDCs largely rescued the abnormally elevated expression of IRF5 and consequently downmodulated expressions of IL-6, TNF-α, IFN-α, and IFN-β genes and CXCR3 protein to the level of those in wild-type pDCs (Fig. 6A–C). Because IRF5 activation directly induces proinflammatory cytokines (33), we hypothesized that the elevated IRF5 by TRAF5 deficiency may cause the highly activated phenotype of *Traf5*$^{-/-}$ pDCs. We thus knocked down IRF5 gene in *Traf5*$^{-/-}$ pDCs by a short-hairpin-RNA method. As expected, IRF5 knockdown in *Traf5*$^{-/-}$ pDCs expressing IRF5 shRNA (shIRF5) suppressed the increased expression of proinflammatory genes observed in *Traf5*$^{-/-}$ pDCs (knockout or control) (Fig. 6D). More importantly, IRF5 shRNA-expressing *Traf5*$^{-/-}$ pDCs expressed normal levels of CXCR3 (Fig. 6E). Collectively, TRAF5 plays a crucial role in inflammatory responses and migratory function of pDCs probably by controlling IRF5 expression in pDCs.

Discussion

Although TRAF5 has important regulatory functions in T and B lymphocytes (17, 36), there is, to date, little understanding of how TRAF5 controls physiological functions of other cell types. In this study, we found that a massive accumulation of pDCs was observed in the skin of *Traf5*$^{-/-}$ mice and that TRAF5 regulated the function of peripheral pDCs by limiting the expression of a skin-tropic chemokine receptor CXCR3 and TLR7/9-induced inflammatory gene expression, which are mediated by IRF5 expression and activation. Thus, in this study, we have uncovered a previously unknown regulatory function of TRAF5 in pDCs that may be relevant for the skin wound healing.

One possible explanation for the enhanced wound healing responses in *Traf5*$^{-/-}$ mice would be caused by the increased expression of CXCR3 in *Traf5*$^{-/-}$ pDCs, which can support the accumulation of circulating pDCs into the inflamed skin tissues. A C-X-C chemokine receptor, CXCR3 is involved in cell migration

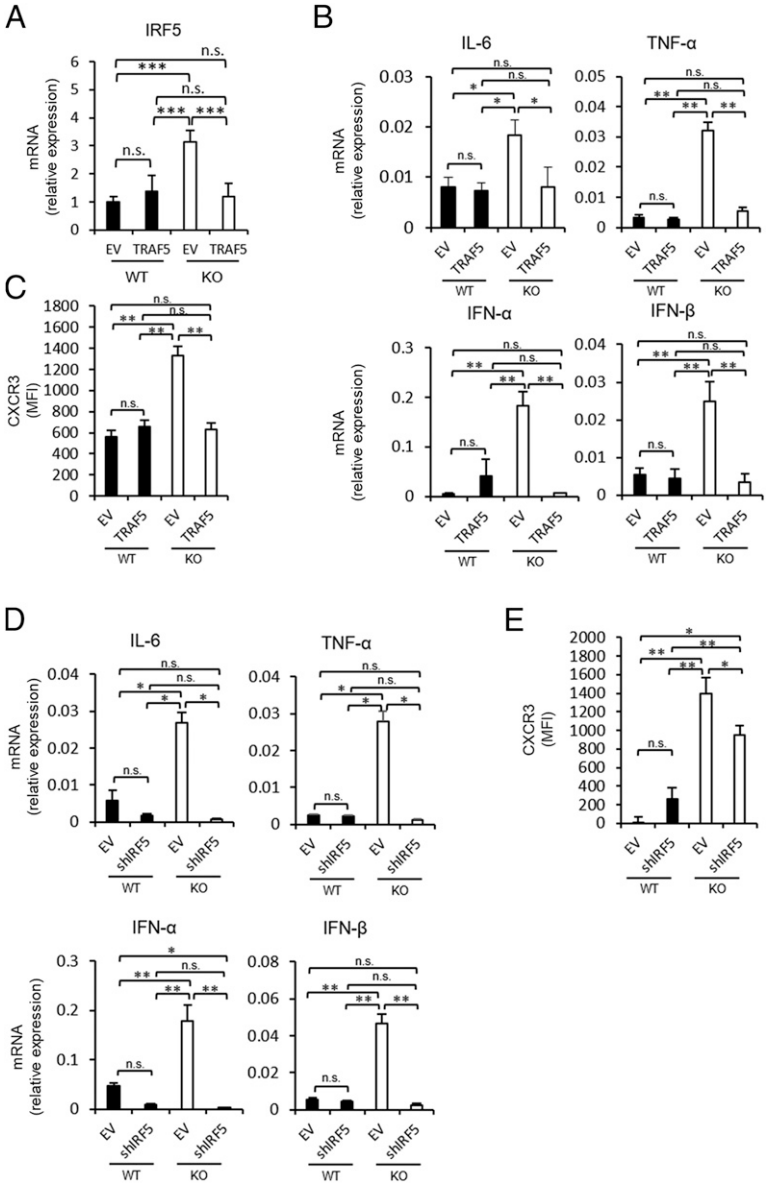

FIGURE 6. TRAF5 negatively regulate expression of IRF5 and CXCR3. (**A**–**C**) Wild-type (WT) and knockout (KO) Flt3L-pDCs transduced by an empty lentiviral vector or TRAF5-expressing lentivirus were sorted as GFP-positive cells by FACS. Expression levels of IRF5 mRNA was quantified by real-time PCR (A), and expression levels of CXCR3 was evaluated by FACS (B). Sorted GFP-positive cells were treated with 5 μg/ml of CpG for 6 or 18 h, and expression levels of IL-6, TNF-α, IFN-α, and IFN-β mRNAs were quantified by real-time PCR (C), and the data are presented as mean ± SD. (**D** and **E**) Control and IRF5-knockdown WT and KO Flt3L-pDCs were stimulated by 5 μg/ml of CpG for 6 or 18 h, and expression of IL-6, TNF-α, IFN-α, and IFN-β was analyzed by real-time PCR (D). These experiments were repeated three times, and data shown as mean ± SD of three replicates were analyzed by Student *t* test. $*p < 0.05$, $**p < 0.01$, $***p < 0.001$.

into inflamed sites via binding to IFN-γ–inducible chemokine ligands, such as CXCL9, CXCL10, and CXCL11 (37–40), and the expression of CXCR3 plays an important role in controlling the function of macrophages and pDCs (26–28, 41, 42). Indeed, CXCR3-deficient mice exhibited impaired skin wound healing responses (43). Our flow cytometric analysis clearly demonstrated that *Traf5*$^{-/-}$ pDCs displayed increased CXCR3 as compared with wild-type pDCs. Although some controversies exist regarding the functional outcome of the interaction between CXCR3 receptor and its ligands (26, 27, 44), we could confirm an important function of CXCR3 expressed by pDCs for cell migration using *trans*-well migration assay. In our model, IFN-γ–stimulated mouse embryonic fibroblast cells may produce any factors other than CXCR3 ligands, but migration of pDCs via CXCR3 is presumed to be functional, as it was blocked by inhibiting CXCR3 by treatment of AMG487. Additionally, administration of CXCR3 inhibitor AMG487 strongly blocked skin wound healing responses.

The ability of pDCs to sense skin injury during wound healing has been reported (16). pDCs accumulate at the inflamed site in response to cathelicidin peptides secreted from injured skin tissues and produced high amount of type I IFN, leading to promoting skin wound healing (16). In the study, cathelicidin peptides were shown to be secreted by injured tissues ∼24 h after wounding. However, our results demonstrated that pDCs migrated into wounded area in *Traf5*$^{-/-}$ mice just within 3 h after wounding. Therefore, enhanced pDC accumulation in the skin of *Traf5*$^{-/-}$ mice may not be explained by cathelicidin secretion in terms of time course. We found high expression of CXCR3 on *Traf5*$^{-/-}$ pDCs. Because keratinocytes produce ligands of CXCR3, such as CXCL9, CXCL10, and CXCL11 (45, 46), TRAF5-controlled accumulation of pDC might be dependent on CXCR3 ligands rather than cathelicidin.

We found that in vitro exogenous expression of TRAF5 in *Traf5*$^{-/-}$ pDC population recovered normal expression of CXCR3 as compared with that on wild-type pDCs. In addition, IRF5 knockdown in *Traf5*$^{-/-}$ pDCs significantly downregulated CXCR3 expression, suggesting a regulatory role of TRAF5 in CXCR3 expression, that is, in part, IRF5 dependent. Thus, this is a new finding showing the functional link between TRAF5 and IRF5 in immune responses. However, further analysis is needed to elucidate the relationships.

TRAF family molecules play important roles in TLR signaling pathways. pDCs, which selectively equip TLR7 and TLR9, produce type I IFN in response to viral invasion and contribute to clearance of virus (6–9). pDCs can also secrete both proinflammatory and anti-inflammatory cytokines by sensing virus- and self-derived nucleic acids (9–11). TRAF3 serves as a critical TLR adaptors and regulates downstream regulatory kinases important for IRF7 activation to induce type I IFN (47). TRAF6 also required for the activation of IRF5 and IRF7 via signalosome, including MyD88 and IRAKs, to induce inflammatory cytokines (30–32, 34, 35, 48). TRAF5 expressed by B cells negatively regulates TLR7/9-mediated IL-6 and TNF-α production and ERK/JNK signaling by controlling the association of TAB2 with TRAF6 without affecting proliferation, survival, and NF-κB activation (36). In this study, as previously shown in *Traf5*$^{-/-}$ B cells, we demonstrated that *Traf5*$^{-/-}$ pDCs also produced higher amounts of IL-6 and TNF-α in response to ligands for TLR7 and TLR9. Interestingly, *Traf5*$^{-/-}$ pDCs displayed increased expression of IRF5, but not IRF7, in steady-state and after TLR stimulation (data not shown). IRF5 positively regulates proinflammatory cytokines IL-6 and TNF-α (29, 31). Actually, IRF5 knockdown in *Traf5*$^{-/-}$ pDCs led to normal expression of inflammatory genes as compared with wild-type pDCs (Fig. 6D). Thus, it is tempting to speculate that TRAF5 negatively controls signaling activity of IRF5 downstream of TLR7/9 in pDCs, which may be critical for augmenting IRF5-driven inflammatory events mediated by pDCs.

In summary, we have revealed an important molecular function of TRAF5 that regulates pDC activity via CXCR3 and IRF5. This study demonstrates a novel mechanism in skin inflammation and wound repair and will provide a new therapeutic approach for the treatment of inflammatory and autoimmune diseases.

Acknowledgments

We thank Hiroyasu Nakano, Makoto Tsuda, and Hidetoshi Tozaki-Saitoh for the gift of essential materials. We also thank the Biomedical Research Core and the Institute for Animal Experimentation (Tohoku University Graduate School of Medicine) for technical support.

Disclosures

The authors have no financial conflicts of interest.

References

1. Eming, S. A., T. Krieg, and J. M. Davidson. 2007. Inflammation in wound repair: molecular and cellular mechanisms. *J. Invest. Dermatol.* 127: 514–525.
2. Wilgus, T. A. 2008. Immune cells in the healing skin wound: influential players at each stage of repair. *Pharmacol. Res.* 58: 112–116.
3. Gurtner, G. C., S. Werner, Y. Barrandon, and M. T. Longaker. 2008. Wound repair and regeneration. *Nature* 453: 314–321.
4. Gallucci, R. M., P. P. Simeonova, J. M. Matheson, C. Kommineni, J. L. Guriel, T. Sugawara, and M. I. Luster. 2000. Impaired cutaneous wound healing in interleukin-6-deficient and immunosuppressed mice. *FASEB J.* 14: 2525–2531.
5. DiPietro, L. A., M. Burdick, Q. E. Low, S. L. Kunkel, and R. M. Strieter. 1998. MIP-1alpha as a critical macrophage chemoattractant in murine wound repair. *J. Clin. Invest.* 101: 1693–1698.
6. Siegal, F. P., N. Kadowaki, M. Shodell, P. A. Fitzgerald-Bocarsly, K. Shah, S. Ho, S. Antonenko, and Y. J. Liu. 1999. The nature of the principal type 1 interferon-producing cells in human blood. *Science* 284: 1835–1837.
7. Gilliet, M., W. Cao, and Y. J. Liu. 2008. Plasmacytoid dendritic cells: sensing nucleic acids in viral infection and autoimmune diseases. *Nat. Rev. Immunol.* 8: 594–606.
8. Swiecki, M., and M. Colonna. 2015. The multifaceted biology of plasmacytoid dendritic cells. *Nat. Rev. Immunol.* 15: 471–485.
9. Swiecki, M., and M. Colonna. 2010. Unraveling the functions of plasmacytoid dendritic cells during viral infections, autoimmunity, and tolerance. *Immunol. Rev.* 234: 142–162.
10. Lande, R., J. Gregorio, V. Facchinetti, B. Chatterjee, Y. H. Wang, B. Homey, W. Cao, Y. H. Wang, B. Su, F. O. Nestle, et al. 2007. Plasmacytoid dendritic cells sense self-DNA coupled with antimicrobial peptide. *Nature* 449: 564–569.
11. Takagi, H., K. Arimura, T. Uto, T. Fukaya, T. Nakamura, N. Choijookhuu, Y. Hishikawa, and K. Sato. 2016. Plasmacytoid dendritic cells orchestrate TLR7-mediated innate and adaptive immunity for the initiation of autoimmune inflammation. *Sci. Rep.* 6: 24477.
12. Banchereau, J., and V. Pascual. 2006. Type I interferon in systemic lupus erythematosus and other autoimmune diseases. *Immunity* 25: 383–392.
13. Rönnblom, L., and G. V. Alm. 2001. An etiopathogenic role for the type I IFN system in SLE. *Trends Immunol.* 22: 427–431.
14. Gilliet, M., and R. Lande. 2008. Antimicrobial peptides and self-DNA in autoimmune skin inflammation. *Curr. Opin. Immunol.* 20: 401–407.
15. Di Domizio, J., A. Blum, M. Gallagher-Gambarelli, J. P. Molens, L. Chaperot, and J. Plumas. 2009. TLR7 stimulation in human plasmacytoid dendritic cells leads to the induction of early IFN-inducible genes in the absence of type I IFN. *Blood* 114: 1794–1802.
16. Gregorio, J., S. Meller, C. Conrad, A. Di Nardo, B. Homey, A. Lauerma, N. Arai, R. L. Gallo, J. Digiovanni, and M. Gilliet. 2010. Plasmacytoid dendritic cells sense skin injury and promote wound healing through type I interferons. *J. Exp. Med.* 207: 2921–2930.
17. Nagashima, H., Y. Okuyama, A. Asao, T. Kawabe, S. Yamaki, H. Nakano, M. Croft, N. Ishii, and T. So. 2014. The adaptor TRAF5 limits the differentiation of inflammatory CD4(+) T cells by antagonizing signaling via the receptor for IL-6. *Nat. Immunol.* 15: 449–456.
18. Masuda, T., S. Iwamoto, R. Yoshinaga, H. Tozaki-Saitoh, A. Nishiyama, T. W. Mak, T. Tamura, M. Tsuda, and K. Inoue. 2014. Transcription factor IRF5 drives P2X4R+-reactive microglia gating neuropathic pain. *Nat. Commun.* 5: 3771.
19. Tanno, H., K. Kawakami, M. Ritsu, E. Kanno, A. Suzuki, R. Kamimatsuno, N. Takagi, T. Miyasaka, K. Ishii, Y. Imai, et al. 2015. Contribution of invariant natural killer T cells to skin wound healing. *Am. J. Pathol.* 185: 3248–3257.
20. Yang, B., J. Suwanpradid, R. Sanchez-Lagunes, H. W. Choi, P. Hoang, D. Wang, S. N. Abraham, and A. S. MacLeod. 2017. IL-27 facilitates skin wound healing through induction of epidermal proliferation and host defense. *J. Invest. Dermatol.* 137: 1166–1175.

21. Tomasek, J. J., G. Gabbiani, B. Hinz, C. Chaponnier, and R. A. Brown. 2002. Myofibroblasts and mechano-regulation of connective tissue remodelling. *Nat. Rev. Mol. Cell Biol.* 3: 349–363.
22. Ramirez, H., S. B. Patel, and I. Pastar. 2014. The role of TGFβ signaling in wound epithelialization. *Adv. Wound Care (New Rochelle)* 3: 482–491.
23. Boniakowski, A. E., A. S. Kimball, A. Joshi, M. Schaller, F. M. Davis, A. denDekker, A. T. Obi, B. B. Moore, S. L. Kunkel, and K. A. Gallagher. 2018. Murine macrophage chemokine receptor CCR2 plays a crucial role in macrophage recruitment and regulated inflammation in wound healing. *Eur. J. Immunol.* 48: 1445–1455.
24. Homey, B., H. Alenius, A. Müller, H. Soto, E. P. Bowman, W. Yuan, L. McEvoy, A. I. Lauerma, T. Assmann, E. Bünemann, et al. 2002. CCL27-CCR10 interactions regulate T cell-mediated skin inflammation. *Nat. Med.* 8: 157–165.
25. Rees, P. A., N. S. Greaves, M. Baguneid, and A. Bayat. 2015. Chemokines in wound healing and as potential therapeutic targets for reducing cutaneous scarring. *Adv. Wound Care (New Rochelle)* 4: 687–703.
26. Vanbervliet, B., N. Bendriss-Vermare, C. Massacrier, B. Homey, O. de Bouteiller, F. Brière, G. Trinchieri, and C. Caux. 2003. The inducible CXCR3 ligands control plasmacytoid dendritic cell responsiveness to the constitutive chemokine stromal cell-derived factor 1 (SDF-1)/CXCL12. *J. Exp. Med.* 198: 823–830.
27. Kohrgruber, N., M. Gröger, P. Meraner, E. Kriehuber, P. Petzelbauer, S. Brandt, G. Stingl, A. Rot, and D. Maurer. 2004. Plasmacytoid dendritic cell recruitment by immobilized CXCR3 ligands. *J. Immunol.* 173: 6592–6602.
28. Brewitz, A., S. Eickhoff, S. Dähling, T. Quast, S. Bedoui, R. A. Kroczek, C. Kurts, N. Garbi, W. Barchet, M. Iannacone, et al. 2017. $CD8^+$ T cells orchestrate pDC-$XCR1^+$ dendritic cell spatial and functional cooperativity to optimize priming. *Immunity* 46: 205–219.
29. Tamura, T., H. Yanai, D. Savitsky, and T. Taniguchi. 2008. The IRF family transcription factors in immunity and oncogenesis. *Annu. Rev. Immunol.* 26: 535–584.
30. Shrivastav, M., and T. B. Niewold. 2013. Nucleic acid sensors and type I interferon production in systemic lupus erythematosus. *Front. Immunol.* 4: 319.
31. Takaoka, A., H. Yanai, S. Kondo, G. Duncan, H. Negishi, T. Mizutani, S. Kano, K. Honda, Y. Ohba, T. W. Mak, and T. Taniguchi. 2005. Integral role of IRF-5 in the gene induction programme activated by toll-like receptors. *Nature* 434: 243–249.
32. Schoenemeyer, A., B. J. Barnes, M. E. Mancl, E. Latz, N. Goutagny, P. M. Pitha, K. A. Fitzgerald, and D. T. Golenbock. 2005. The interferon regulatory factor, IRF5, is a central mediator of toll-like receptor 7 signaling. *J. Biol. Chem.* 280: 17005–17012.
33. Ban, T., G. R. Sato, A. Nishiyama, A. Akiyama, M. Takasuna, M. Umehara, S. Suzuki, M. Ichino, S. Matsunaga, A. Kimura, et al. 2016. Lyn kinase suppresses the transcriptional activity of IRF5 in the TLR-MyD88 pathway to restrain the development of autoimmunity. *Immunity* 45: 319–332.
34. Ning, S., J. S. Pagano, and G. N. Barber. 2011. IRF7: activation, regulation, modification and function. *Genes Immun.* 12: 399–414.
35. Honda, K., and T. Taniguchi. 2006. Toll-like receptor signaling and IRF transcription factors. *IUBMB Life* 58: 290–295.
36. Buchta, C. M., and G. A. Bishop. 2014. TRAF5 negatively regulates TLR signaling in B lymphocytes. *J. Immunol.* 192: 145–150.
37. Dai, Z., L. Xing, J. Cerise, E. H. Wang, A. Jabbari, A. de Jong, L. Petukhova, A. M. Christiano, and R. Clynes. 2016. CXCR3 blockade inhibits T cell migration into the skin and prevents development of alopecia areata. *J. Immunol.* 197: 1089–1099.
38. Wenzel, J., S. Lucas, S. Zahn, S. Mikus, D. Metze, S. Ständer, E. von Stebut, U. Hillen, T. Bieber, and T. Tüting. 2008. CXCR3 <-> ligand-mediated skin inflammation in cutaneous lichenoid graft-versus-host disease. *J. Am. Acad. Dermatol.* 58: 437–442.
39. Croudace, J. E., C. F. Inman, B. E. Abbotts, S. Nagra, J. Nunnick, P. Mahendra, C. Craddock, R. Malladi, and P. A. Moss. 2012. Chemokine-mediated tissue recruitment of CXCR3+ CD4+ T cells plays a major role in the pathogenesis of chronic GVHD. *Blood* 120: 4246–4255.
40. Lee, J. H., B. Kim, W. J. Jin, H. H. Kim, H. Ha, and Z. H. Lee. 2017. Pathogenic roles of CXCL10 signaling through CXCR3 and TLR4 in macrophages and T cells: relevance for arthritis. *Arthritis Res. Ther.* 19: 163.
41. Butler, K. L., E. Clancy-Thompson, and D. W. Mullins. 2017. $CXCR3^+$ monocytes/macrophages are required for establishment of pulmonary metastases. *Sci. Rep.* 7: 45593.
42. Zhou, J., P. C. Tang, L. Qin, P. M. Gayed, W. Li, E. A. Skokos, T. R. Kyriakides, J. S. Pober, and G. Tellides. 2010. CXCR3-dependent accumulation and activation of perivascular macrophages is necessary for homeostatic arterial remodeling to hemodynamic stresses. *J. Exp. Med.* 207: 1951–1966.
43. Yates, C. C., D. Whaley, P. Kulasekeran, W. W. Hancock, B. Lu, R. Bodnar, J. Newsome, P. A. Hebda, and A. Wells. 2007. Delayed and deficient dermal maturation in mice lacking the CXCR3 ELR-negative CXC chemokine receptor. *Am. J. Pathol.* 171: 484–495.
44. Krug, A., R. Uppaluri, F. Facchetti, B. G. Dorner, K. C. Sheehan, R. D. Schreiber, M. Cella, and M. Colonna. 2002. IFN-producing cells respond to CXCR3 ligands in the presence of CXCL12 and secrete inflammatory chemokines upon activation. *J. Immunol.* 169: 6079–6083.
45. Bünemann, E., N. P. Hoff, B. A. Buhren, U. Wiesner, S. Meller, E. Bölke, A. Müller-Homey, R. Kubitza, T. Ruzicka, A. Zlotnik, et al. 2018. Chemokine ligand-receptor interactions critically regulate cutaneous wound healing. *Eur. J. Med. Res.* 23: 4.
46. Richmond, J. M., D. S. Bangari, K. I. Essien, S. D. Currimbhoy, J. R. Groom, A. G. Pandya, M. E. Youd, A. D. Luster, and J. E. Harris. 2017. Keratinocyte-derived chemokines orchestrate T-cell positioning in the epidermis during vitiligo and may serve as biomarkers of disease. *J. Invest. Dermatol.* 137: 350–358.
47. Oganesyan, G., S. K. Saha, B. Guo, J. Q. He, A. Shahangian, B. Zarnegar, A. Perry, and G. Cheng. 2006. Critical role of TRAF3 in the toll-like receptor-dependent and -independent antiviral response. *Nature* 439: 208–211.
48. Ning, S., A. D. Campos, B. G. Darnay, G. L. Bentz, and J. S. Pagano. 2008. TRAF6 and the three C-terminal lysine sites on IRF7 are required for its ubiquitination-mediated activation by the tumor necrosis factor receptor family member latent membrane protein 1. *Mol. Cell. Biol.* 28: 6536–6546.